ON THE MODELLING OF LEAK RATES THROUGH CRACKS IN PIPES AND TUBES

by

S.I. Osamusali, K. Crentsil, R.Y. Chu and J.C. Luxat
Nuclear Safety Department
Ontario Hydro H11 B17
700 University Avenue
Toronto, Ontario M5G 1X6

ABSTRACT

A leak rate code, LEAK-RATE Version 1.0, has been developed to predict two-phase critical mass fluxes, exit pressures and pressure profiles for cracks, which forms an integral part of leak-before-break (LBB) analysis of pressurized reactor components such as pipes and headers. The code can also be used to calculate steam generator tube leakages. LEAK-RATE Version 1.0 code uses the homogeneous frozen model (HFM) for determining critical mass flux, with effects of friction accounted for within the crack. The code predictions have been compared with an extensive experimental database, and also benchmarked against other similar international codes. The code predicted the leak rates and exit pressures to within ±25% of experimental data, which represents a reasonably good agreement for leak rate predictions. The predicted pressure profiles within the crack agreed well with experimental data and yielded the same trend as the experimental observations.

1.0 INTRODUCTION

Nuclear plants are designed to safely shutdown in the event of a sudden pipe rupture. To satisfy pipe break criteria, the plants require pipe whip restraints and jet impingement shields. These structures are expensive and impede access for in-service inspection and maintenance as well as increase radiation exposure of personnel. The leak-before-break (LBB) analysis is being used to demonstrate that a through-wall pipe crack produces a detectable leakage well in advance of an unstable crack growth that could result in sudden catastrophic pipe rupture. The ability to detect a leakage long before a crack becomes unstable provides an alternative approach to satisfying pipe break criteria, thus preventing the need for complex and costly design measures to protect against pipe rupture dynamic effects, such as pipe whip and jet impingement. As part of LBB analysis, leak rates through cracks are determined to provide a correlation with the crack sizes for determining the margin to attain the critical crack size.

Under typical nuclear reactor operating conditions, the leakage flow through cracks can flash into vapour. The compressible two-

phase crack flow may exhibit critical flow or choking. Thus, a two-phase critical flow model is needed to treat leakages through cracks. An earlier version of the code, LEAK-RATE Version 0.0 [1] was developed to correlate measured leak rates to crack sizes, while experimental investigation was being conducted at Ontario Hydro Research Division (OHRD) [2].

This paper presents LEAK-RATE Version 1.0 [3] code, which modifies and extends the range of applicability of Version 0.0, for predicting leak rates through various pipes and tube-wall cracks. LEAK-RATE Version 1.0 accounts for changes in mass flux due to variations in the crack cross-sectional area, and sharp entrance pressure drops. It uses the Bernoulli equation for calculating single-phase discharges and includes various crack geometries. Several models have been proposed for calculating critical two-phase flow discharges from pipe cracks. The suitability of these models depends on the fluid conditions and the geometry under consideration. The homogeneous frozen model (HFM), developed for fluid and geometrical conditions similar to those expected for leakages through a crack in heat transport piping, is widely reported in the literature. This model has been chosen for the present study due to its simplicity, and its tendency to yield good predictions of the critical mass flux [4]. In addition, the model requires very few parameters to be correlated, making it more mechanistically viable. The main disadvantage of the homogeneous frozen model is its dependence on fluid conditions at the choking plane, which are usually unknown. Henry and Fauske [5] have derived a form of the HFM model that depends only on the stagnation conditions. For long cracks, however, frictional pressure drops in the crack which may become significant, were not considered in their model. In the present analysis, the effects of friction has been included, hence the HFM equation given by Whalley [4] will be applied at the crack throat, after solving the mass and momentum equations, assuming homogeneous equilibrium flow, for the pressure drop along the crack and the thermalhydraulic conditions at the throat. The critical flow and the pressure drop equations, together, form a set of non-linear equations, which can be numerically solved for the critical mass flux and exit-plane pressure.

A Homogeneous Non-Equilibrium Model (HNEM) is also being developed in parallel with the HFM. The HNEM is a lumped parameter model based on a non-equilibrium critical flow model [6], to be used separately as a scoping tool to provide initial guesses for the HFM model. The HFM model, which uses a nodalized flow path, yields the crack-path pressure profiles, exit-plane pressures and the crack discharge mass-flow rate.

The leak rate code described in this work was developed to provide leak rate estimates for given crack sizes. An extensive database, including data from an on-going experimental program at OHRD [2], on experimental leak rates, was established and used to

validate LEAK-RATE Version 1.0 [3]. The code predictions were further compared against those of internationally available codes such as SQUIRT (BATTELLE/IPIRG) [7] and PICEP (EPRI) [8].

2.0 **CRITICAL FLOW MODELS**

It has been well established that choking or critical flow of a single-phase fluid occurs when the following condition is attained:

$$1 + G_c^2\left(\frac{\partial v}{\partial p}\right)_s = 0 \qquad (1)$$

where G_c is the critical mass flux, v is the specific volume, p is the pressure and s represents the entropy. Equation (1) has been derived from a momentum balance with an assumption of frictionless flow, and for conditions corresponding to an infinitely large pressure gradient. This frictionless flow assumption has been stated to be valid as the flow becomes choked or nearly choked [4].

2.1 **Homogeneous Frozen Model (HFM)**

The homogeneous frozen model to be applied at the crack throat can be derived from Equation (1) based on the following assumptions:

(i) The flow is homogeneous and average phase velocities are equal (i.e., no slip).

(ii) Choking occurs at the crack exit.

(iii) The quality is frozen at the choking plane.

(iv) The vapour expands isentropically as an ideal gas.

(v) The flow is adiabatic.

(vi) The liquid phase is incompressible.

Therefore, for a single component two-phase flow (e.g., steam-water flow), the HFM can be derived from Equation (1), based on the above assumptions, by expressing the two-phase specific volume as,

$$v = xv_g + (1-x)\,v_l \qquad (2)$$

where x represents the quality, v_g and v_l represent the specific volumes of the vapour and liquid phases, respectively. Substituting Equation (2) into (1) yields:

$$1 + G_c^2 x \left(\frac{\partial v_g}{\partial p} \right)_s = 0 \qquad (3)$$

By invoking the fourth assumption stated above, we obtain,

$$\left(\frac{\partial v_g}{\partial p} \right)_s = - \frac{v_g}{\gamma p} \qquad (4)$$

where, γ=1.33, represents the ratio of specific heats. The two-phase critical mass flux based on the HFM then becomes,

$$G_c = \sqrt{\left(\frac{\gamma p_t}{x_t v_{gt}} \right)} \qquad (5)$$

The subscript t has been inserted to indicate that the critical mass flux is evaluated based on the fluid conditions at the choking plane (or throat).

Assuming adiabatic flow, the thermodynamic quality, x_t can be expressed as:

$$x_t = \frac{h_o - h_{ft}}{h_{fgt}} \qquad (6)$$

where h_o, h_{ft} and h_{fgt} represent the stagnation, liquid and latent enthalpies, respectively. The liquid and latent enthalpies, as well as the vapour specific volume can be determined using the property subroutines (i.e., equation of state). In this study, the property subroutines have been taken from the SOPHT code [9].

The validity of the one-dimensional flow assumption for constant area rectangular channels is supported by the crack-path pressure measurements of OHRD [2]. Divergent/convergent channels, however, tend to exhibit two-dimensional effects. The flow-path geometry representative of a through-wall crack in a pipe is shown in Figure 1.

In the present analysis, frictional pressure drop is assumed to be dominant, especially for long cracks. Additional pressure drops due to changes in the fluid density, entrance effects, obstructions and other appendages may also be significant. These effects are accounted for in the total pressure drop expression given as:

$$\Delta p = \left(\frac{1}{C^2} + \frac{fL}{D} + \Sigma_i \, k_i \right) \frac{G^2}{2\rho} \tag{7}$$

Equation (7) represents a sum of the entrance, frictional and obstruction pressure drops, respectively. Accelerational pressure drop resulting from density changes, when flashing to a two-phase mixture occurs, is accounted for by continuously updating both the fluid density and the pressure drop from the property subroutine, at each node in the numerical scheme. In this procedure, both the inlet and outlet pressures of the node are evaluated and an average density based on these pressures determined.

The constant C represents the orifice contraction coefficient. The value of C may vary with the geometry of the crack and the flow rate. For a rectangular orifice with a sharp entrance the orifice coefficient, C is 0.61, at conditions applicable to those under consideration in which the approach velocity to the crack entrance is nearly zero, and the stagnation chamber dimensions are much larger than the crack opening. Although, a rounding off of the entrance may lead to higher values of C, the default value of 0.61 has been used throughout for consistency. In practice, the crack entrance is expected to be quite sharp. k_i represents the pressure drop coefficient due to various obstructions and appendages along the crack, L represents the pipe-wall thickness, and D is the hydraulic diameter. For turbulent flows in cracks with rough walls, an explicit form of the Colebrook and White friction factor correlation developed by Swamee and Jain [10] has been applied, namely,

$$f = \frac{1}{\left[2 \log \left(\frac{\varepsilon}{3.7D} + \frac{5.74}{Re^{0.9}} \right) \right]^2} \tag{8}$$

where ε is the average roughness height, and Re represents the Reynolds number. This friction factor correlation has been chosen because it requires no iteration in f, and also accounts for Reynolds number dependence. The two-phase viscosity is expressed as:

$$\frac{1}{\mu} = \frac{x}{\mu_g} + \frac{(1-x)}{\mu_l} \qquad (9)$$

where μ_l and μ_g are the liquid and vapour dynamic viscosities, respectively. The viscosities, and densities are evaluated at the average node pressure, with the enthalpy remaining constant at the stagnation value. The density is given as, $\rho = 1/v$, where v is given by Equation (2). The fluid properties at the crack throat are evaluated based on the stagnation enthalpy and the throat pressure, determined by solving Equations (6) to (9). Equation (5) is then applied at the crack throat (or choking plane) to estimate the critical mass flux.

2.2 Homogeneous Non-Equilibrium Model (HNEM)

The critical flow model described here is a one-dimensional homogeneous non-equilibrium model, modified from the original model by Henry [6] to include effects of wall friction, flow area changes, and flow path bends and obstructions [11].

The homogeneous non-equilibrium critical flow model can be derived from Equation (1) based on the same set of assumptions stated in Section 2.1, except that the flow is not frozen in this case. Also negligible vapor formation is assumed in a region defined by $0 \leq L/D < 12$.

Following the derivation of the HFM critical mass flux (Section 2.1), the HNEM critical mass flux becomes,

$$G_c^2 = \frac{1}{\left[x\frac{v_g}{\gamma p} - (v_g - v_{lo})\,N\frac{dx_E}{dp}\right]_t} \qquad (10)$$

In Equation (10), the term $N(dx_E/dp)$ replaces dx/dp according to Henry [6], and $v_l = v_{lo}$, since the liquid phase is incompressible. v_{lo} is the stagnation liquid specific volume, x_E is the equilibrium quality and N is the Henry non equilibrium parameter. The subscript, t signifies that the quantity in bracket is evaluated at the crack throat conditions.

The non-equilibrium parameter, N is given by,

$$N = \begin{cases} 20x_E, & x_E < 0.05 \\ 1, & x_E \geq 0.05 \end{cases}$$

The exit plane quality is expressed by Henry [6] as;

$$x_t = Nx_E \left[1 - e^{-B\left(\frac{L}{D}-12\right)}\right] \qquad (11)$$

where B = 0.0523, L is the crack depth and D is the crack opening displacement. The above expression represents the rate at which vapour generation approaches its equilibrium value from metastability. Note that when N = 0, Equation 10 represents the homogeneous frozen model (HFM - see Equation 3) and when N = 1, it yields the homogeneous equilibrium model (HEM).

In this case, the throat pressure is obtained from the crack path pressure drop according to:

$$p_t = p_o - \Delta p \qquad (12)$$

where p_o is the stagnation pressure and p_t is the exit plane pressure. ΔP consists of several components as expressed below,

$$\Delta P = \Delta P_e + \Delta P_f + \Delta P_{aa} + \Delta P_{ap} + \Delta P_k$$

ΔP_e = entrance pressure drop
ΔP_f = frictional pressure drop
ΔP_{aa} = accelerational pressure drop due to area change
ΔP_{ap} = accelerational pressure drop due to phase change
ΔP_k = pressure drop due to crack path bends/protrusions

3.0 **NUMERICAL SOLUTION**

A double-iterative-method in both the pressure and mass flux is applied to Equation (7) to determine both the pressure and flow conditions at the throat. An initial guess of the mass flux is made, and the two-phase critical mass flux given by Equation (5) is used as the closure condition. Continuous testing for the initial guess which would yield a rapid convergence is being conducted.

Since flashing may not readily occur for highly subcooled cases, numerical problems may be encountered with the closure condition (i.e., critical flow expression) given by Equation (5) for low guesses of the initial mass flux, since the crack pressure drop will be greatly underpredicted giving a zero quality. Equation (5) was therefore re-written as:

$$G_c = \sqrt{\left(\frac{\gamma p_t}{v}\right)} \tag{13}$$

to be used as the closure condition if the throat quality remains zero while still iterating for the critical mass flux. If, however, convergence has been obtained in the mass flux, while the throat quality remains zero, it implies that flashing did not occur in the crack, and the two-phase critical flow solution is simply replaced with a discharge flow rate determined from the expression,

$$G = \sqrt{\left(\frac{2\rho_o\,(p_o - p_{amb})}{\frac{1}{C^2} + \frac{fL}{D} + \Sigma_i\, k_i}\right)} \tag{14}$$

where p_o and ρ_o represent the pressure and density of the stagnation conditions, respectively, and p_{amb} represents the ambient pressure.

3.1 **Numerical Procedure**

For a given crack geometry and fluid stagnation conditions:

1) Estimate mass flux, G.

2) Iterate on node pressure and thermodynamic properties to get consistent converged values.

3) Using final throat conditions from iteration loop 1, evaluate mass flux G_c from Equation (5). If $G_c \neq G(1\pm\sigma)$ then adjust G and repeat. σ represents the tolerance.

For cases where $x_t=0$ due to a low guess of the mass flux, the critical mass flux is calculated from Equation (13). Upon attaining convergence in the mass flux, the critical two-phase flow rate would have been obtained if the throat quality is greater than zero. Otherwise, the single-phase discharge flow rate is calculated using Equation (14).

Relative convergence criteria have been used in the LEAK-RATE code for both the node outlet pressure and mass flux. For the pressure, we have:

$$\left| \frac{p^i - p^{i-1}}{p^i} \right| \leq \sigma \qquad (15)$$

where i represents the i-th iteration and σ is the tolerance. Similarly, for the mass flux we have:

$$\left| \frac{G^i - G^{i-1}}{G^i} \right| \leq \sigma \qquad (16)$$

A tolerance of 1% was used for both the exit pressures of the nodes and the discharge mass flux, since this was found to yield convergent solutions.

4.0 **RESULTS AND DISCUSSION**

4.1 **Summary of Test Cases**

The predictions of LEAK-RATE Version 1.0 have been compared against limited experimental data for both artificial and real pipe cracks available in the open literature. Comparisons have also been made against experimental data for artificial rectangular cracks obtained at Ontario Hydro Research Division (OHRD) [2]. Comparisons are made mainly for mass flow rates, but, where data are available, the throat pressures and pressure profiles have also been compared. The various data used for the current validation are summarized in Table 1.

4.1.1 **Code-to-Code Comparison**: Code-to-code comparisons were also made using results from PICEP, an Electric Power Research Institute (EPRI) code [8], applied to OHRD experimental data for artificial cracks, and from SQUIRT, an International Piping Integrity Research Group (IPIRG) code [7], applied to both EPRI Phases I and II experimental data for artificial and real cracks [12], respectively. The comparison of LEAK-RATE code results with those of SQUIRT and PICEP codes has also been conducted using Amos and Schrock data for artificial cracks [13]. All three codes yielded the same range of prediction accuracy with experimental data.

In a separate study, these experimental data were also used to compare with the predictions of the homogeneous non-equilibrium model (HNEM) described in Section 2.2, and the agreement obtained were quite similar to those of LEAK-RATE Version 1.0. A subsequent study is planned to incorporate the HNEM critical mass flux expression given in Equation (10) as an alternate closure

condition in the LEAK-RATE Version 1.0 code. The stagnation properties and geometrical parameters for each set of experiment used for comparison are fully stated in Table 1.

4.2 **OHRD Data [2]**

A comparison of LEAK-RATE Version 1.0 predictions with the leak rate data of Fixture SS-A1 is shown in Figure 2. The results show that LEAK-RATE Version 1.0 predicts the experimental data to within ±25%. A comparison of the result obtained with the PICEP code for the same set of data is given by OHRD [2] as shown in Figure 3, and the results yielded a similar agreement to the LEAK-RATE Version 1.0 predictions.

The nodalization procedure used in the solution scheme of LEAK-RATE Version 1.0 enables the determination of pressure profile and subsequently flashing in the crack. A typical pressure profile has been compared with OHRD experimental data for Fixture SS-A1 in Figure 4, and reasonably good agreement exists between the predictions and the experimental result (solid circular symbols). LEAK-RATE Version 1.0 also accounts for sharp entrance pressure drops. As could be seen from Figure 4, the sharp entrance geometry tends to yield a rather high pressure drop close to the crack entrance.

Further comparisons have been made between the code predictions and the experimental data for Fixtures SS-A2 and SS-A3. Figures 5 to 7 show the results for Fixture SS-A3 having the same geometry as Fixture SS-A1 but with a higher COD. In this case, the LEAK-RATE Version 1.0 predictions are within ±25% of the experimental data (Figure 5), and a reasonably good agreement was obtained for the pressure profiles given in Figure 7. Again, LEAK-RATE Version 1.0 yielded similar agreement with the PICEP code predictions of the same experimental data in Figure 6.

Figures 8 to 10 show the results obtained for the straight rectangular crack sample (Fixture SS-A2). The results show that the code predicts the experimental leak rates to within +50% and -25% (Figure 8), representing a fairly good agreement. A typical experimental pressure profile obtained for this sample was also compared with the code predictions in Figure 10 where reasonably good agreement was also obtained. The PICEP code predictions of the same set of leak rate data have been presented in Figure 9, which shows similar agreement to LEAK-RATE Version 1.0 predictions.

4.3 **EPRI Data [12]**

LEAK-RATE Version 1.0 predictions have also been compared to the experimental data of EPRI Phase I for artificial cracks. The

results obtained have been presented in Figures 11 to 14. Figure 11 shows the LEAK-RATE Version 1.0 code predictions of the experimental data to be within +50% and -25% of the experimental data. Apparently, plugging problems from particulates in the unfiltered water supply probably originating from carbon steel surfaces of the vessel used, were encountered during the experiment. A comparison of the SQUIRT code predictions of the same set of experimental data yields agreement within +40% and -60% (see Figure 12).

The measured exit pressures of the EPRI Phase I test have also been compared with predictions of LEAK-RATE Version 1.0 in Figure 13, and agrees with experimental data to within ±25%. A comparison of the code prediction of the pressure profile with the measured pressures along the crack, for stagnation pressure of 3260 kPa, and temperature of 227.8°C, presented in Figure 14, yields good agreement.

The code was also compared to EPRI Phase II experimental real crack data in Figures 15 and 16. Figure 15 shows the comparison of LEAK-RATE Version 1.0 code predictions with the measured leak rates with the results predicted to within ±25%. In a code-to-code comparison with the SQUIRT code predictions of the same experimental data, approximately the same range of agreement was obtained, since the SQUIRT code predictions were within ±30% (Figure 16).

4.4 **Amos and Schrock Data [13]**

LEAK-RATE Version 1.0 code predictions of Amos and Schrock experimental data for smooth rectangular cracks are presented in Figures 17 and 18, and shows agreement to within ±25%. Figure 19 shows a comparison of the SQUIRT code predictions with the experimental data for cracks with CODs ranging from 0.127 mm to 0.381 mm, which also includes the set of data used to validate LEAK-RATE Version 1.0. The SQUIRT code is seen to predict the data to within 0 to -70%, representing a poorer agreement than the LEAK-RATE predictions. The predictions of LEAK-RATE Version 1.0 for exit pressures of the sample with a COD of 0.381 mm is seen to be better than ±25% (Figure 20).

4.5 **Sources of Discrepancies**

The discrepancies between the code predictions and experimental data may be due to the following factors;

(a) Real crack shapes are usually not well defined. Various geometrical shapes such as rectangular, elliptical, parabolic or diamond could be assumed for the cracks. The crack opening area may differ by as much as a factor of two depending on whether a

rectangular or a diamond shape is assumed for the calculations.

(b) Few experimenters reporting leak rates through cracks fail to provide the characteristics of the inlet geometry. Amos and Schrock [13] have observed that leak rates through rounded entrances tend to be higher than those of sharp entrances. The inlet geometry characteristics are also primary factors in the pressure profile determination.

(c) The crack surface roughness, bends and protrusions are primary factors in leak rate determination. Their dimensions may be comparable to the crack opening displacement thereby increasing the effective crack-flow path. The result of this is an additional pressure drop.

(d) The friction factor correlations presently used were originally developed for circular geometries. These are assumed to be applicable to cracks if the pipe diameter is replaced with the hydraulic diameter of the crack. While the velocity profiles and frictional resistances are well understood for pipes, tight cracks which have widely different cross-sectional shape from that of a circle, may yield secondary flows and invalidate the hydraulic diameter concept.

(e) Particulate plugging of the crack path could reduce the leak rates measured and lead to discrepancies in the code comparisons, affecting the leak-before-break analysis.

(f) Two-phase flow patterns, presently not well understood for cracks, may also be important in modelling cracks, since some of the parameters used in the calculation of pressure drop are flow pattern dependent.

5.0 **CONCLUSION**

The LEAK-RATE Version 1.0 code has been developed based on the homogeneous frozen model (HFM) to predict leakages through cracks at elevated temperature and pressure conditions for various crack openings. The code predictions have been compared to the leak rate measurements performed at the Ontario Hydro Research Division (OHRD) and other leak rate data found in the open literature. The following conclusions have been reached from the results of the present investigation:

1. The code predicted the experimental leak rate and exit pressure data to within ±25%, which represents a reasonably good agreement for leak rate predictions.

2. The OHRD experimental pressure profiles were well predicted by the code for the case where the entrance geometry was assumed to be sharp.

3. Since both rounded and sharp entrance geometries yield significantly different pressure profiles depending on the discharge coefficient used, crack entrance geometries need to be accurately specified to enable the prediction of pressure profiles in the cracks.

4. The code also predicts flashing locations, which are determined from the pressure profiles within the cracks.

5. The code predictions of the experimental leak rate results yielded similar agreement with the predictions of the PICEP and SQUIRT codes.

ACKNOWLEDGEMENT

The authors wish to thank M.T. Flaman and B.E. Mills of Mechanical Research Department, Ontario Hydro, for providing the OHRD experimental data used for the present code validation.

NOMENCLATURE

A	Crack cross-sectional area	(m^2)
a	Crack length or extension	(m)
B	Constant in Equation (11)	(-)
C	Coefficient in Equation (7)	(-)
D	Crack hydraulic diameter	(m)
f	Friction factor	(-)
G	Mass flux	(kg/m^2s)
G_c	Critical mass flux	(kg/m^2s)
h_{ft}	Liquid enthalpy	(kJ/kg)
h_{fgt}	Latent enthalpy	(kJ/kg)
h_o	Stagnation enthalpy	(kJ/kg)
k_1	Coefficient in Equation (7)	(-)
L	Crack depth or pipe thickness	(m)
N	Henry non-equilibrium parameter	(-)
p	Pressure	(N/m^2)
p_{amb}	Ambient pressure	(N/m^2)
p_o	Stagnation pressure	(N/m^2)
p_t	Crack throat pressure	(N/m^2)
Δp	Pressure drop	(N/m^2)
Re	Reynolds number	(-)
T_o	Stagnation temperature	(°C)
v_g	Gas specific volume	(m^3/kg)
v_l	Liquid specific volume	(m^3/kg)
v_{lo}	Liquid specific volume at stagnation condition	(m^3/kg)
x	Quality	(-)
x_E	Equilibrium quality	(-)
x_t	Throat quality	(-)

Greek Symbols

γ	Isenthropic exponent	(-)
δ	Crack centre opening displacement	(m)
ε	Average roughness height	(m)
θ	Crack orientation	(°)
μ	Viscosity	(kg/m.s)
ρ	Density	(k/m^3)
Σ	Summation sign	(-)
σ	Convergence criterion	(-)
τ	Shear stress	(N/m^2)

Superscript

i	ith node
i-1	(i-1)th node

Subscript

aa	accelerational/area
amb	Ambient
ap	accelerational/phase

c	Critical
e	entrance
f	friction
ft	Liquid at throat
fgt	Latent
g	Gas
gt	Gas at throat
i	i-th node
k	bends/protrusions
l	Liquid
o	Stagnation
s	Enthropy
t	Throat
w	Wall

REFERENCES

1. Slongo C. and C.S. Kim, "LEAK-RATE - Code Description and User's Guide", Ontario Hydro, Report No. 89229, September 1989.

2. Boag, J.M., M.T. Flaman and B.E. Mills, "Leak Rate Experiments for Through-Wall Artificial Cracks", Leak-Before-Break in Water Reactor Piping and Vessels, Ed. C.E. Coleman, Elsevier Applied Science, New York (1990).

3. Osamusali, S.I. and K. Crentsil, "LEAK-RATE Version 1.0", Ontario Hydro, Report No. 91354, December, 1991.

4. Whalley, P.B., Boiling, Condensation and Gas-Liquid Flow, Oxford University Press, Oxford (1987).

5. Henry, R.E. and H.K. Fauske, "The Two-Phase Critical Flow of One-Component Mixtures in Nozzles, Orifices and Short Tubes", J. Heat Transfer, Vol. 93, pp 179-187 (1971).

6. Henry, R.E., "The Two-Phase Critical Discharge of Initially Saturated or Subcooled Liquid", Nuclear Science and Engng., Vol. 41, pp 336-342 (1970).

7. Paul, D.D., J. Ahmad, P.M. Scott, L.F. Flannigan and G.M. Wilkowski, "Evaluation and Refinement of Leak-Rate Estimate Models", U.S. NRC Report #NUREG/CR-5128, BMI-2164 (1988).

8. Norris, D., A. Okamoto, B. Chexal and T. Griesbach, "PICEP: Pipe Crack Evaluation Program", EPRI Report # NP-3596-SR, Revision 1 (1987).

9. Chang,Y.F., "A Thermal-Hydraulic System Simulation Model for the Reactor, Boiler and Heat Transport System (SOPHT)", Ontario Hydro Report # CNS 37-2, September, 1977.

10. Swamee, P.K. and A.K. Jain, "Explicit Equations for Pipe-Flow Problems", Proc. A.S.C.E. J. Hydraulics Div., 102, HY5, pp 657-664 (1976).

11. Abdollahian, D. and B. Chexal, "Calculation of Leak Rates Through Pipes and Tubes", EPRI Report No. NP-3395, 1983.

12. Collier, R.P., F.B. Stulen, M.E. Mayfield, D.B. Pape and P.M. Scott, "Two-Phase Flow Through Intergranular Stress Corrosion Cracks and Resulting Acoustic Emission", EPRI Report # NP-3540-LD, Battelle Columbus Lab., April 1984.

13. Amos, C.N. and V.E. Schrock, "Critical Discharge of Initially Subcooled Water Through Slits", U.S. NRC Report # NUREG/CR-3475, September 1983.

Table 1: Thermalhydraulics and Geometrical Input Data for Experimental Fixtures

Reference	Stagnation Condition	Crack Shape	Crack Length (mm)	Crack Outer Width (mm)	COD (mm)	Roughness Height (μm)	Comments
OHRD [2] Fixture SS-A1	p_o=0.8 - 12 MPa T_o=29 - 299°C	Flared 75.2°	38.1	98.6	0.102	0.203	Varying X-section. Exp. Error: 5-10%.
OHRD [2] Fixture SS-A2	p_o=1.2 - 10 MPa T_o=165 - 296°C	Rectan-gular	38.1	48.8	0.109	0.203	Const. X-section. Exp. Error: 5-10%.
OHRD [2] Fixture SS-A3	p_o=1.0 - 12 MPa T_o=166 - 272°C	Flared 75.2°	38.1	98.6	0.508	0.203	Varying X-Section. Exp. Error: 5-10%.
EPRI [12] Phase I Data	p_o=3.3 - 11.5 MPa T_o=178 - 268°C	Rectan-gular	57.15	63.5	0.2 - 1.12	0.3 - 10.2	Artificial Cracks. Errors not reported
EPRI [12] Phase II Data	p_o=4.0 - 9.07 MPa T_o=220 - 282°C	Rectan-gular	17.3	9.53	0.108	0.178	Real cracks. Exp. Errors not given
Amos & Schrock Data [13]	p_o=4.1 - 15.8 MPa T_o=195 - 346°C	Rectan-gular	63.5	20.0	0.381, 0.254	0.0 (smooth)	Smooth surfaces. Exp. Error: 15-20%

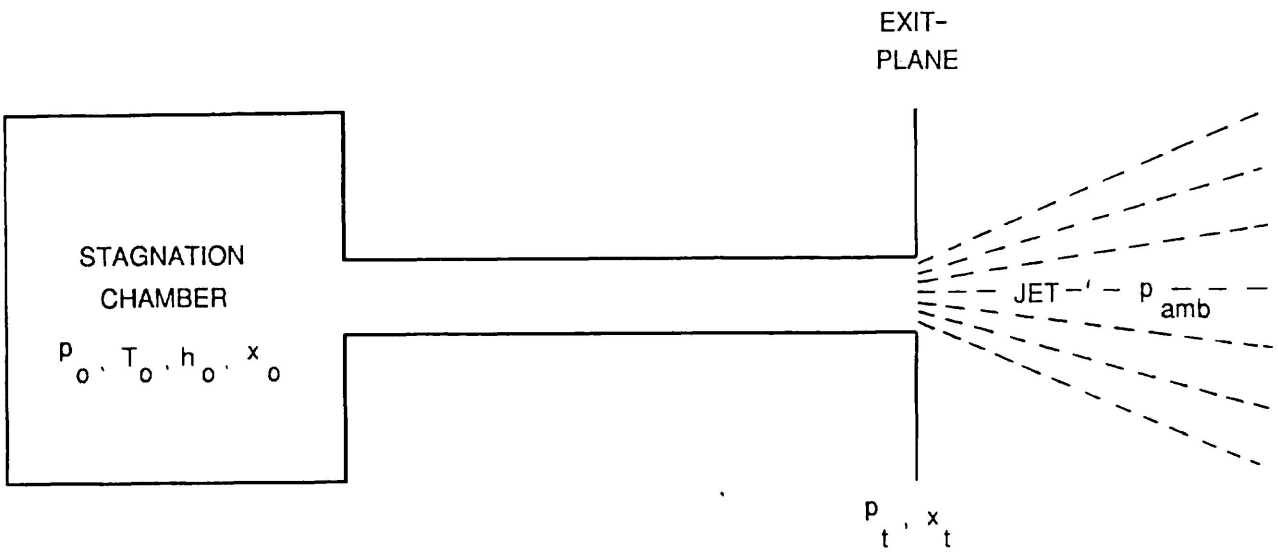

Figure 1
Schematic Diagram of a Through-Wall Pipe Crack

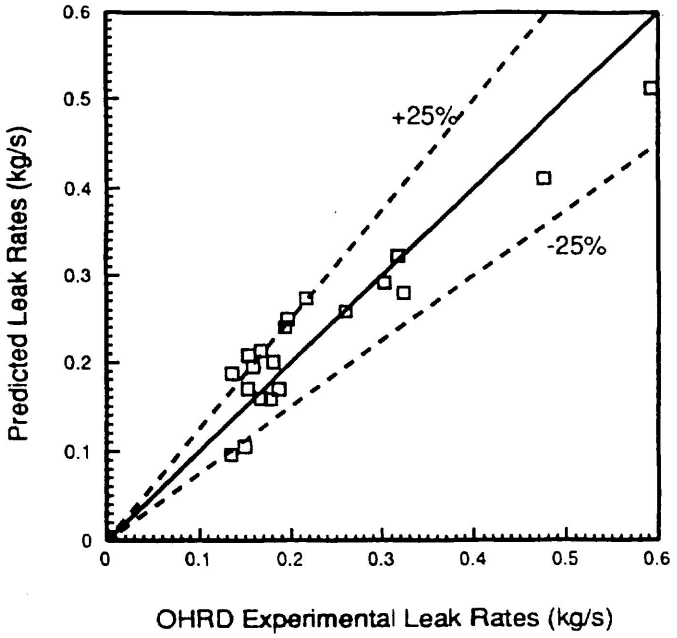

Figure 2
LEAK-RATE Version 1.0 Prediction of OHRD Leak Rate Data for Fixture SS-A1

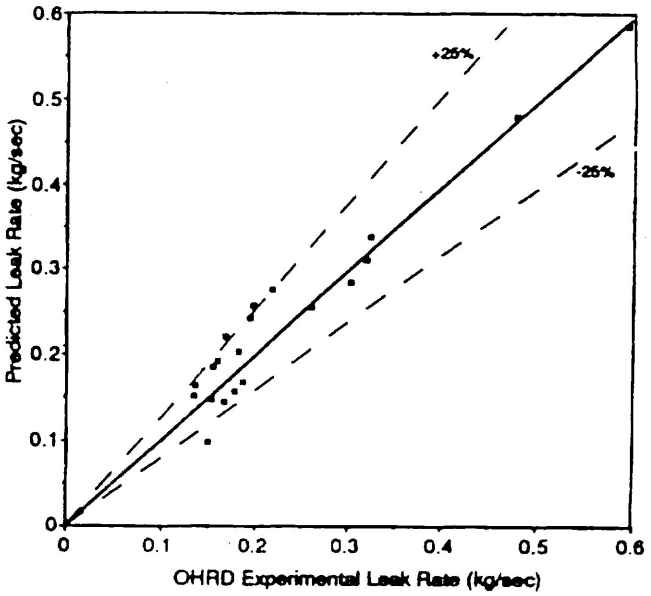

Figure 3
PICEP Code Prediction of OHRD Leak Rate Data for Fixture SS-A1 [2]

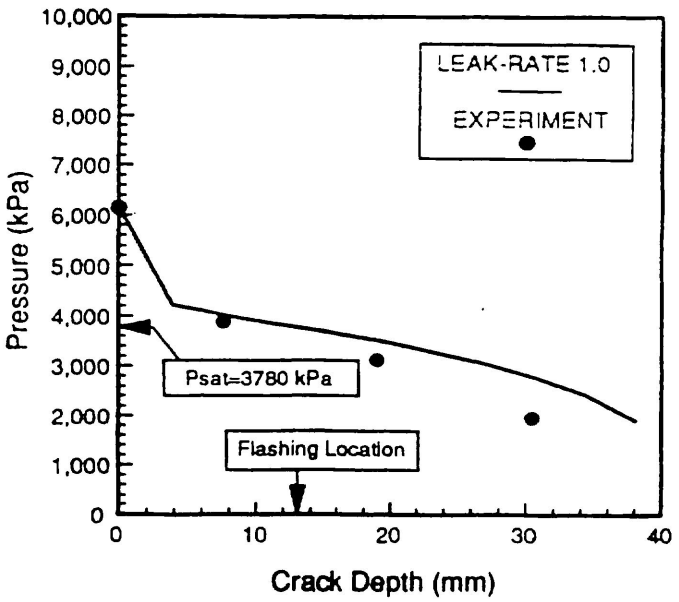

Figure 4
LEAK-RATE Version 1.0 Prediction of OHRD Pressure Profile for Fixture SS-A1
(p_o=6148 kPa, T_o=247°C)

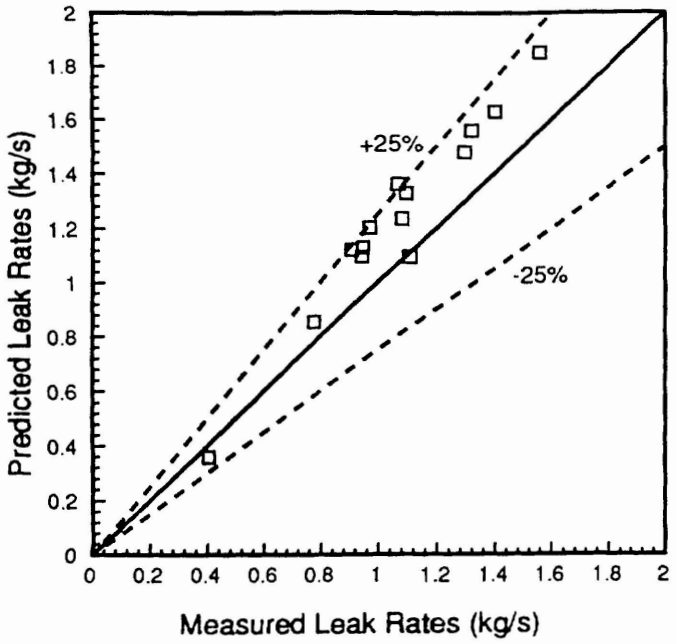

Figure 5
LEAK-RATE Version 1.0 Prediction of OHRD
Leak Rate Data for Fixture SS-A3

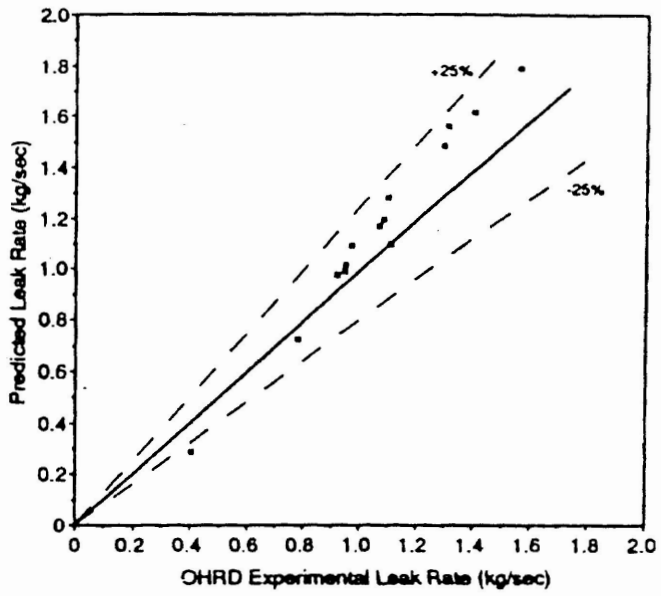

Figure 6
PICEP Code Prediction of OHRD Leak Rate
Data for Fixture SS-A3 [2]

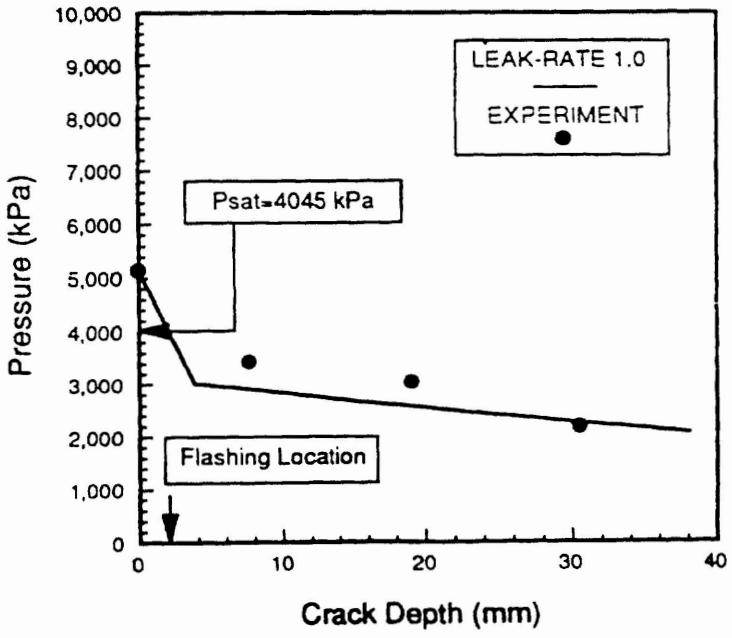

Figure 7
LEAK-RATE Version 1.0 Prediction of OHRD
Pressure Profile for Fixture SS-A3
(p_o=5145 kPa, T_o=251°C)

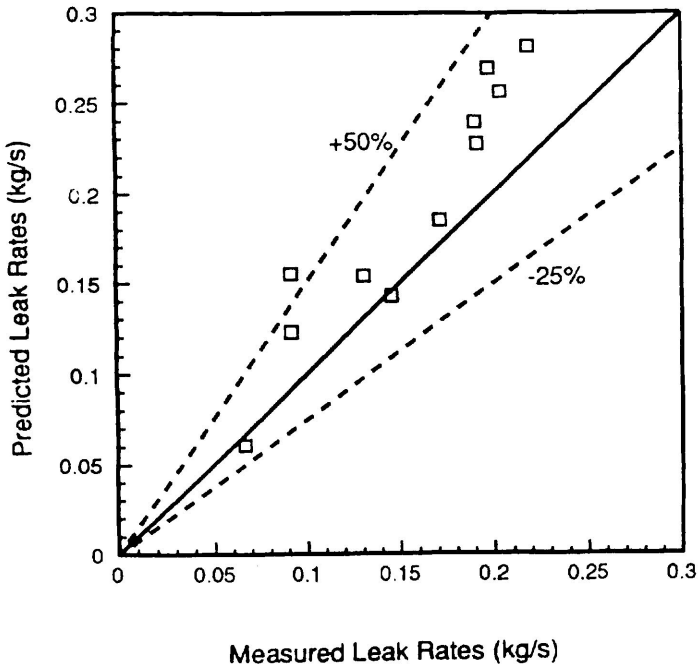

Figure 8
LEAK-RATE Version 1.0 Prediction of OHRD
Leak Rate Data for Fixture SS-A2

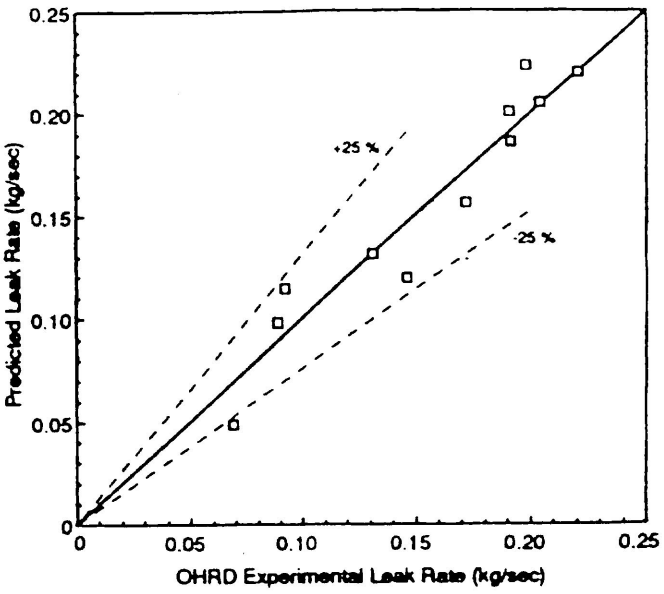

Figure 9
PICEP Code Prediction of OHRD Leak Rate
Data for Fixture SS-A2 [2]

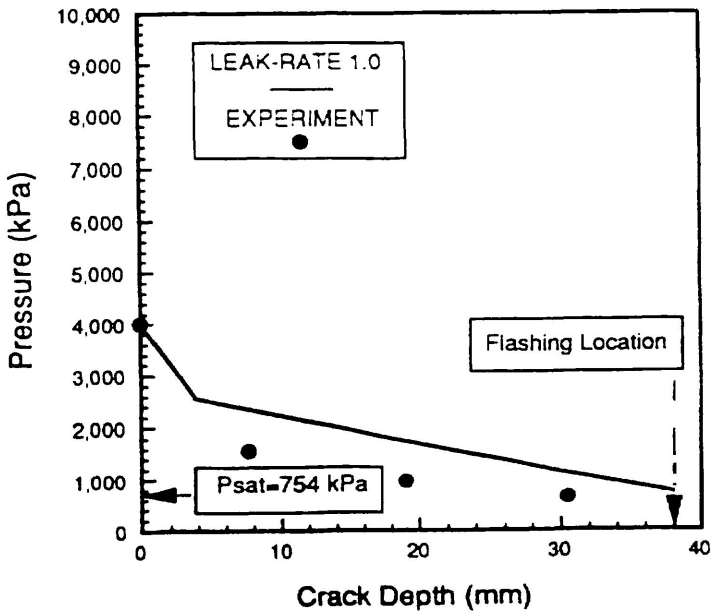

Figure 10
LEAK-RATE Version 1.0 Prediction of OHRD
Pressure Profile for Fixture SS-A2
(p_o=4009 kPa, T_o=168°C)

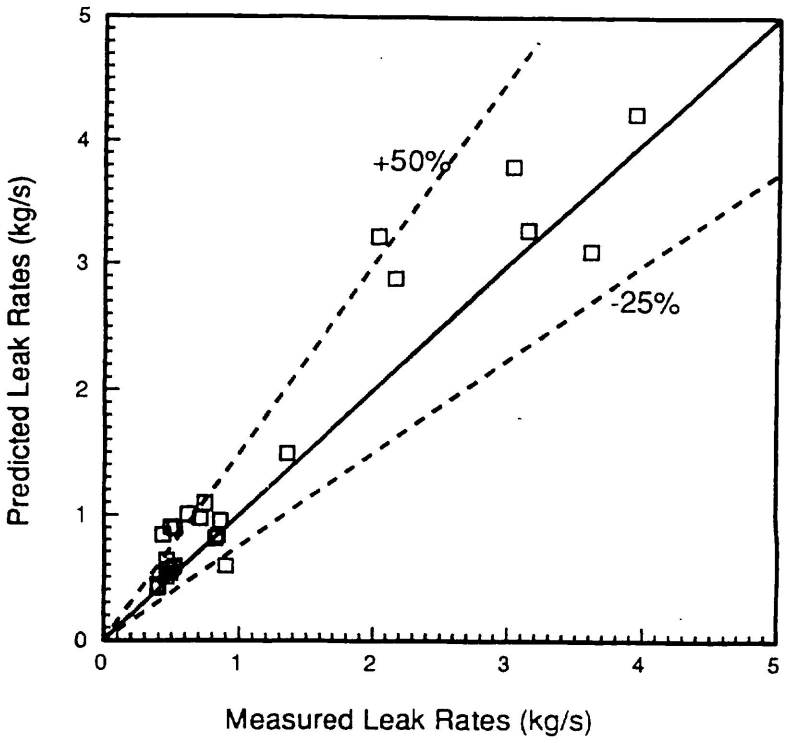

Figure 11
LEAK-RATE Version 1.0 Prediction of EPRI Phase I
Leak Rate Data

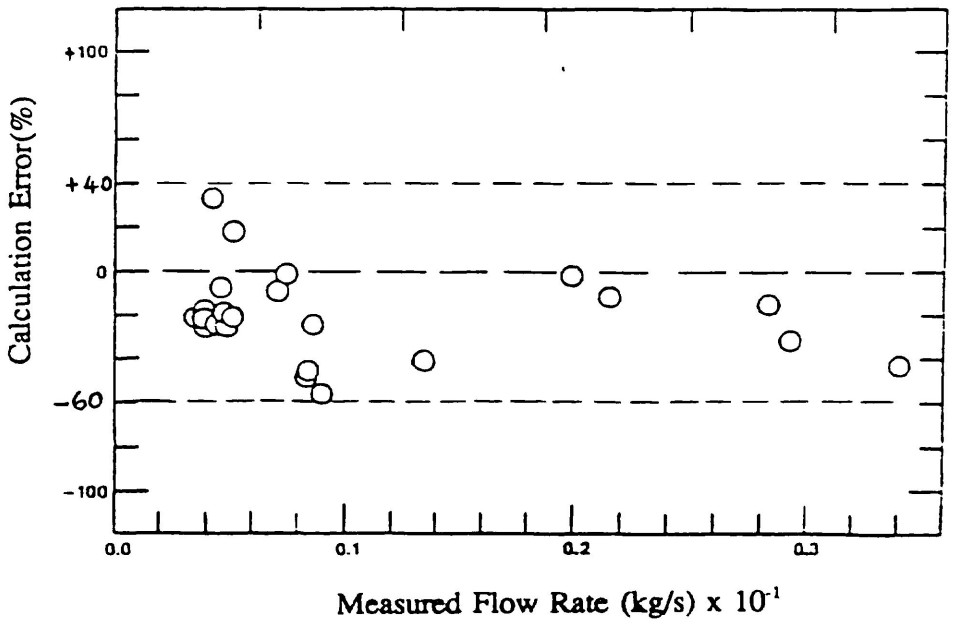

Figure 12
SQUIRT Code Prediction of EPRI Phase I
Leak Rate Data [7]

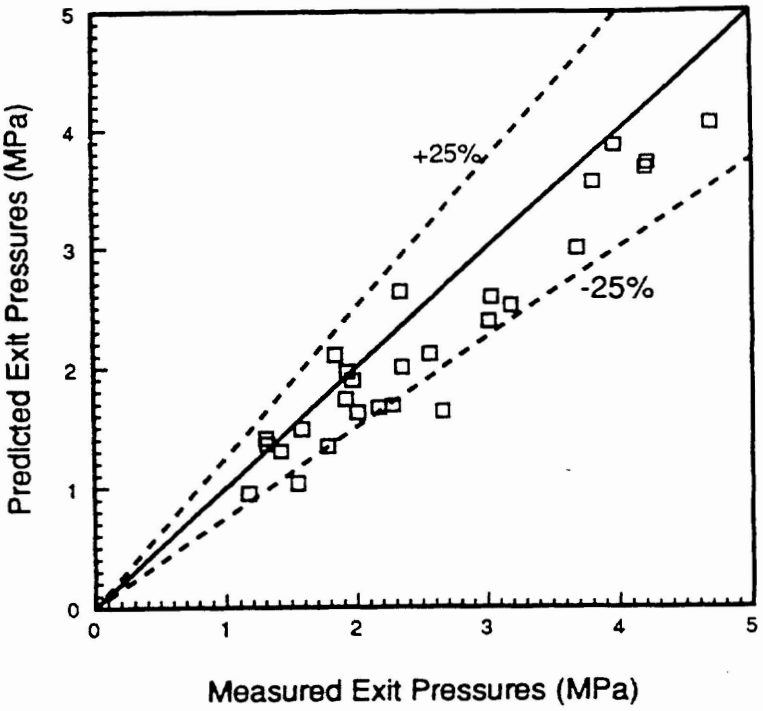

Figure 13
LEAK-RATE Version 1.0 Prediction of EPRI Phase I
Exit Pressure Data

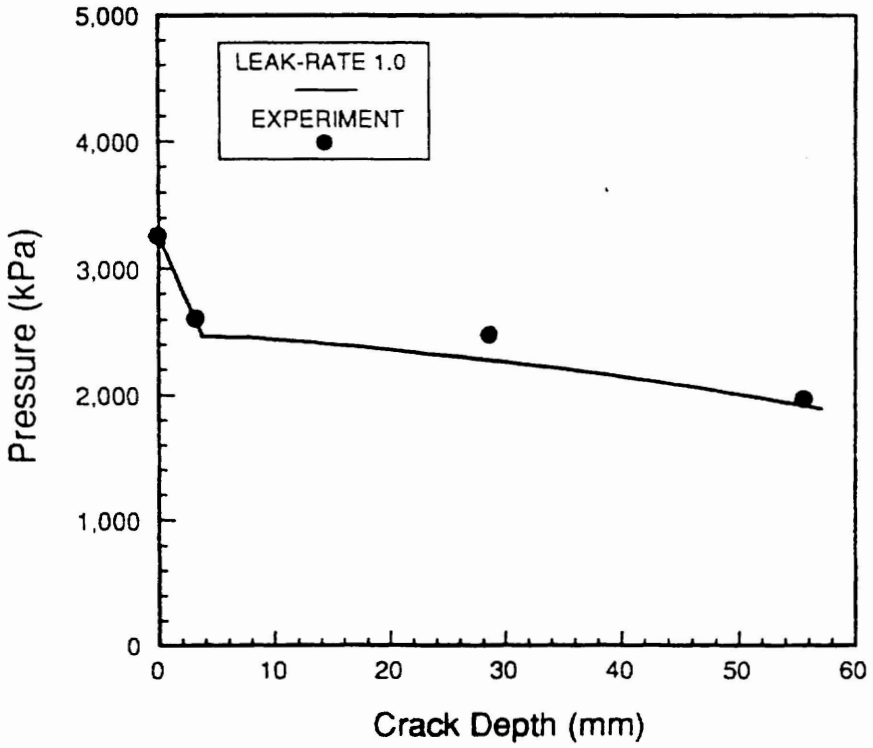

Figure 14
LEAK-RATE Version 1.0 Prediction of EPRI Phase I
Pressure Profile for Run #11
(p_o=3260 kPa, T_o=227.8°C)

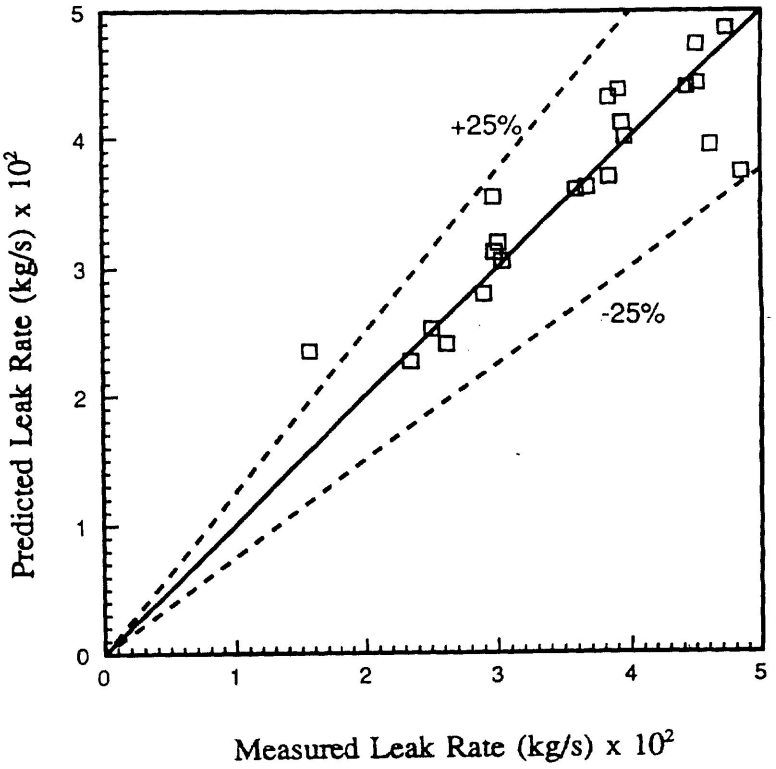

Figure 15
LEAK-RATE Version 1.0 Prediction of EPRI Phase II
Leak Rate Data for COD of 0.108 mm

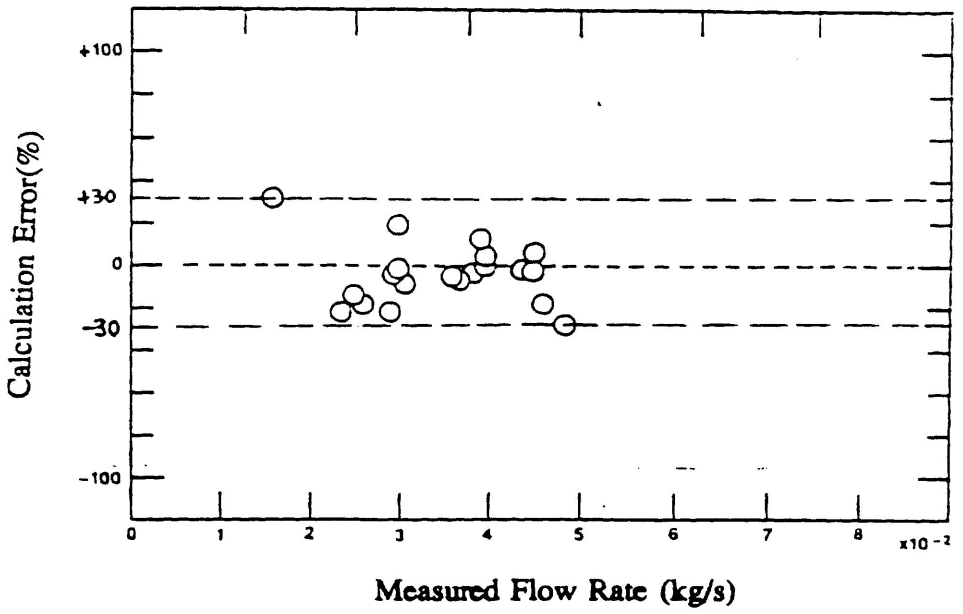

Figure 16
SQUIRT Code Prediction of EPRI Phase II
Leak Rate Data for COD of 0.108 mm [7]

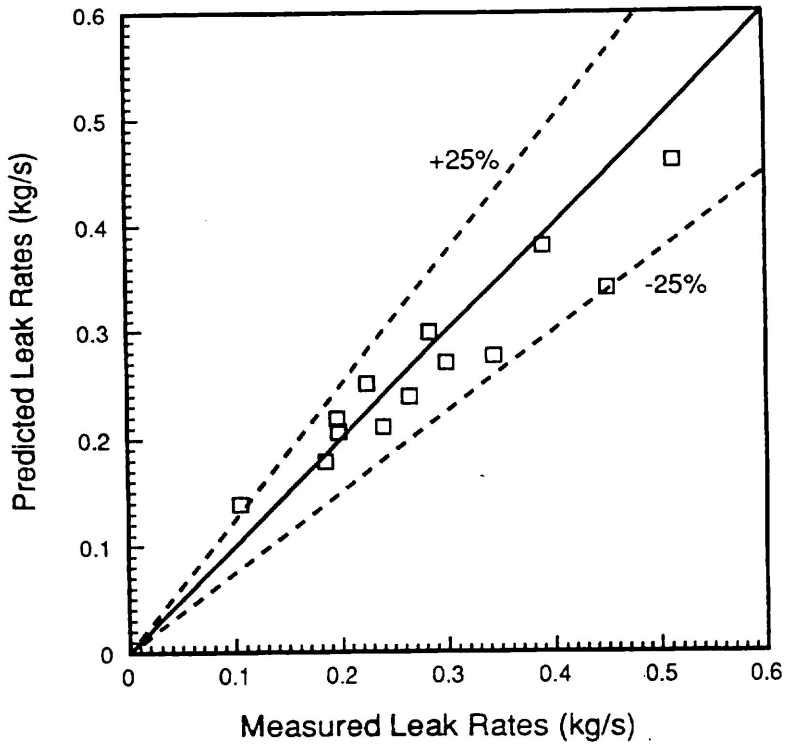

Figure 17
LEAK-RATE Version 1.0 Prediction of Amos and Schrock Leak Rate Data for COD of 0.381 mm

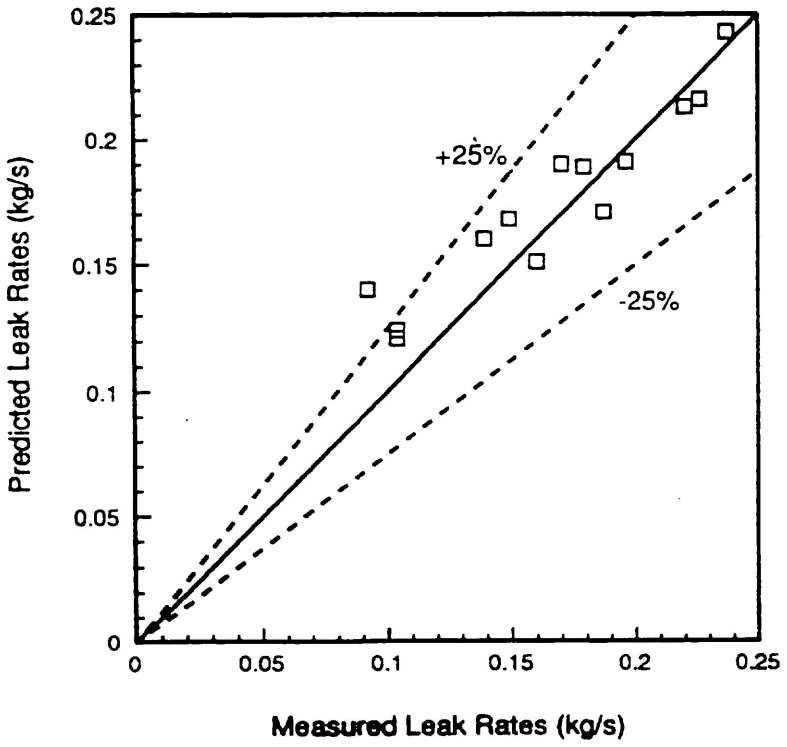

Figure 18
LEAK-RATE Version 1.0 Prediction of Amos and Schrock Leak Rate Data for COD of 0.254 mm

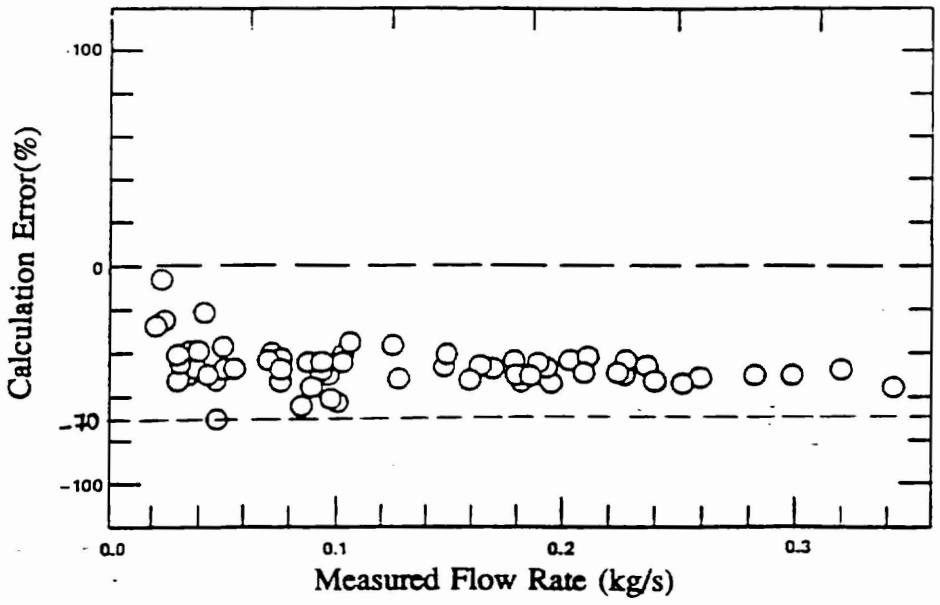

Figure 19
SQUIRT Code Prediction of Amos and Schrock
Leak Rate Data for COD of 0.127 mm to 0.381 mm [7]

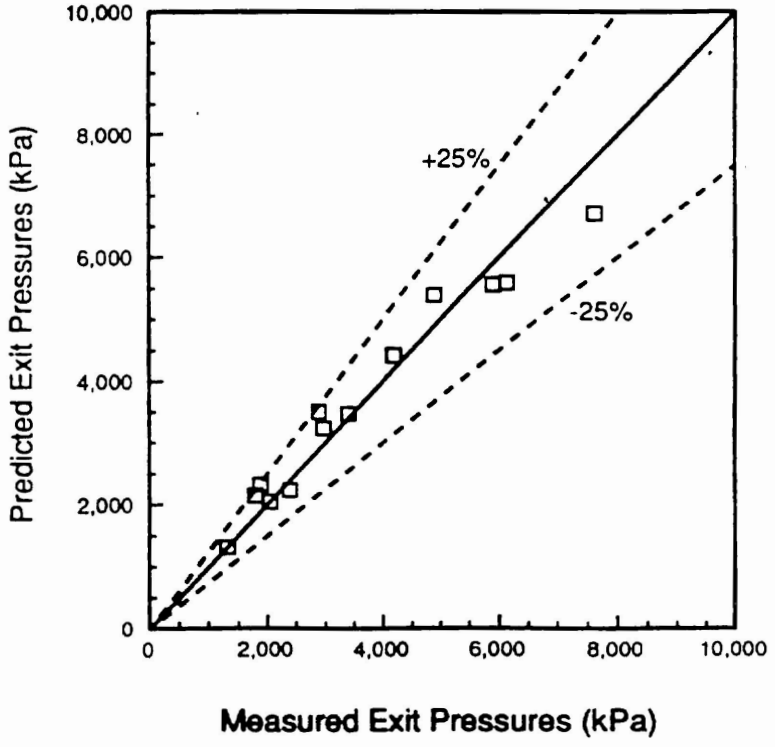

Figure 20
LEAK-RATE Version 1.0 Prediction of Amos and
Schrock Exit Pressure Data for COD of 0.381 mm